MODELLING OF A BAYESIAN SYSTEM FOR ACCURATE ESTIMATION OF BODY TEMPERATURE FROM THERMAL IMAGES

Edward Netzer[1] and Peterson Belan[2]
[1] Informatics and Knowledge Management Post Graduate Program, Nove de Julho University
edward.netzer@gmail.com
[2] Informatics and Knowledge Management Post Graduate Program, Nove de Julho University
pbelan@gmail.com

ABSTRACT

This study presents an innovative methodology for accurately measuring body temperature using market-available thermal cameras and Bayesian networks. It was observed that the precision of temperature measurements from thermal cameras can be significantly improved through this approach. The study started with the acquisition of 460 thermal images, which were processed and analysed using a Bayesian networks algorithm implemented in MATLAB. The errors in directly measuring temperature from the thermal camera were minimized with the use of the proposed methodology, resulting in a significant improvement in accuracy. Although the results are promising, improvements are needed for applications that require more precise temperature measurements, such as health monitoring. The study concludes that the application of Bayesian networks for thermal image analysis presents a potential solution for accurately measuring body temperature and represents an important direction for future research in this area.

KEYWORDS: *Thermal Image, Bayesian networks, Body Temperature, MATLAB, Medical diagnostics*

I. INTRODUCTION

Healthcare professionals face practical challenges in the implementation and monitoring of sensors for body temperature measurement, requiring careful management of these devices, which are typically placed in abdominal or axillary regions [1], [2]. It is imperative that the thermal monitoring system should be safe, minimally invasive, and compatible with other essential medical devices [3].
Temperature measurement is linked to the emission of infrared radiation from a body, first recognized by Sir William Herschel in 1800 [3], [4]. John Herschel, in subsequent works, advanced in this area and coined the term "Thermography", describing the visualization of infrared radiation [4].
Since the introduction of thermography in medicine by Lloyd Williams (1964), there have been significant studies in this area, such as the identification of the emissivity of human skin by Steketee (1973) and the application of thermography in body temperature measurement [5], [6].
Recent research has explored different applications of thermography, including monitoring of respiratory rate based on the temperature profile of the nostrils [3] and temperature detection by [7].
The adoption of computer vision techniques in thermography studies has been notable in recent years, with recent works by [8]–[10]. Although progress has been made in the application of thermography in various areas, there is still a need for additional studies to maximize the potential of this technique for non-contact skin temperature measurement.

1.1. Related Works

The analysis of the temperature profile in the nostril region for monitoring new-borns' breathing using infrared thermography was first described by Abbas et al. (2011) [3]. This study identified challenges reading variations in environmental temperature and the need for improvements on the nasal area detection.

In Knobel-Dail et al. (2017) [11] was used infrared thermography to assess the temperature of premature babies, demonstrating the possibility of detecting body temperature within an incubator with an infrared camera. Despite a variation of about 2°C compared to skin sensors, the study identified changes in blood flow.

Berksoy et al. (2018) [12], measured the temperature on the face and forehead of children using infrared radiation, although without employing thermography. Ornek et al. (2019) [13] applied Infrared Thermography and Convolutional Neural Networks for the first time to detect the health status of new-borns. The study considers the assumption that diseases and infections may cause local temperature changes resulting in thermal asymmetry on the skin surface.

Rodriguez-Lozano et al. (2019) [8] developed a technique for segmentation of the forehead area, enabling the extraction of the average temperature of this region, even with the presence of external elements. In Ammer et al. (2019) [4] has presented a detailed manual for the use of thermography, including medical applications.

Negishi et al. (2020) [9] developed a vital signs measurement system for screening tests in patients with flu, using thermal image processing and RGB images. The system, although not focused on new-borns, provided measurements of heart rate, respiratory rate, and body temperature.

Rassels et al. (2021) [14] proposed a technique for measuring the body temperature of new-borns in an incubator using thermal images, while compensating for offset error with an additional temperature measure. The technique used an additional temperature measurement to compensate the offset error caused by the combination of calibration error and electronic path error of the camera.

Jaddoa et al. (2021) [15] applied computer vision to locate the ocular region of cattle for temperature measurement through thermography. Wang et al. (2021) [16] used infrared thermography, an anemometer, and a humidity meter to measure cattle's temperature, adjusting for environmental factors.

Yang et al. (2022) [10] proposed a system that employs computer vision techniques and convolutional neural networks to measure body temperature and respiratory rate in adults, showing a small difference of less than 0.5°C compared to a portable forehead thermometer.

1.1. Organization of the Paper

Section 2 presents the necessary theoretical background for understanding the techniques used. Section 3 presents the materials and methods used for the development of the work. In section 4 the results obtained are presented as well as the discussion of the results. Finally, in the last section, 5, the conclusion is presented.

II. THEORETICAL BACKGROUND

2.1. Electromagnetic Spectrum

Electromagnetic radiation, including light, is produced by the agitation of particles with an electric charge, such as segments of molecules in a heated state. The light perceptible to humans represents a section of the electromagnetic spectrum, which also encompasses other types of electromagnetic radiation [17].

This electromagnetic spectrum starts with gamma and X-rays, goes through ultraviolet rays, advances to visible light (from the violet color to the red), continues to infrared radiation, microwaves, radio waves of different lengths, and culminates in long radio waves (JUNG et. al. 2008).

Radiation is released in discrete quantities of energy called photons, which have a dual nature - particle and wave. The main characteristic to distinguish the ranges of the electromagnetic spectrum is the wavelength, which is the distance between consecutive peaks of irradiated energy. The energy level of photons is defined by their wavelength, indicated by the Greek letter lambda (λ), and expressed in length units (m).

In Figure 1, it can be seen that photons with high energy have shorter wavelengths and higher frequencies, while photons with low energy have longer wavelengths and lower frequencies. In the intermediate range of the spectrum, one can identify the thermal radiation that covers part of the ultraviolet rays, all the visible light spectrum, and part of the infrared spectrum.

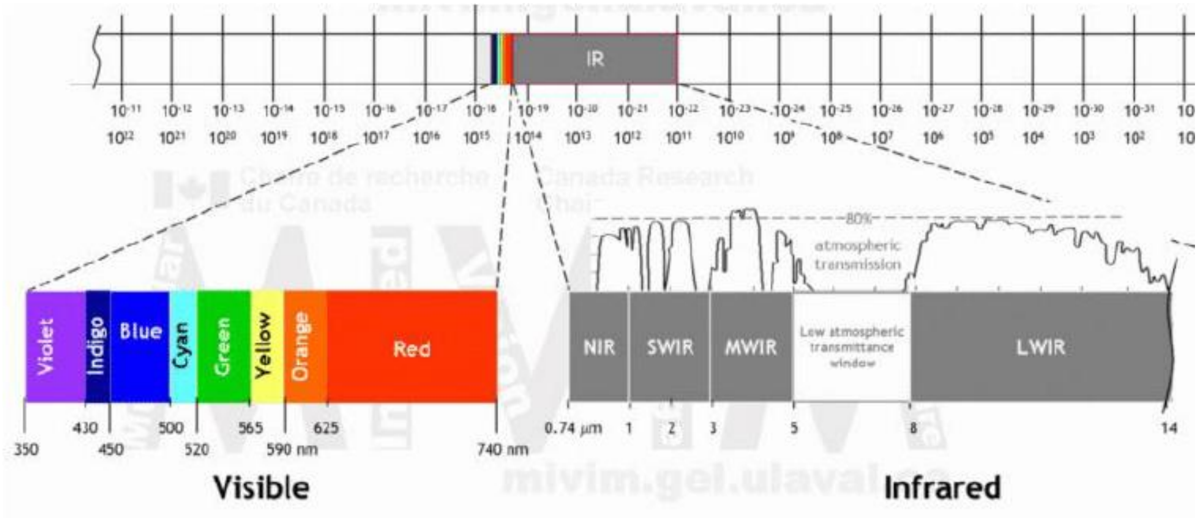

Figure 1. Electromagnetic spectrum showing the visible and infrared wavelength intervals [18]

Additionally, there is a breakdown of the visible light spectrum, indicating the wavelengths corresponding to each color interval. In the infrared spectrum, the highlight is the LWIR range (Long Wave Infrared), which goes from 8µm to 14µm, an interval that includes the 8µm to 12µm range, encompassing the emissions from the human body normally measured for diagnoses, as indicated by [3].

2.2. Infrared Radiation and Human Skin Emissivity

The infrared radiation emitted by the human body is in the range of 8 to 12µm [3]. The human skin, with an emissivity of 0.98, minimally reflects the infrared radiation from other heat sources present in the environment, characterizing itself almost as a black body, which absorbs all incident radiation [19]. Emissivity remains constant for the propagation of the electromagnetic wave up to 45° from the normal angle to the surface of the observed object. However, if this angle is increased, there may be variations in emissivity and increases in the measurement error, requiring some form of compensation [14].

Studies show that human skin is a near-perfect radiator, with emissivity very close to that of a black body. On the other hand, the effect of different skin pigmentation on emissivity is still unknown, although recent studies have indicated that pigmentation does not seem to significantly influence thermal emissivity [20].

The measurement of body temperature can be impacted by the reflected radiation coming from the ambient temperature. However, due to the high emissivity of human skin, the reflection of the ambient temperature is minimal. In the case of skin treated with ointments, gels, or solutions, possible changes in emissivity should be considered to avoid significant errors in the measurements if the reflected ambient temperature is very different from the temperature of the analysed tissue [19].

2.3. Infrared Thermography

Infrared thermography cameras allow the detection of infrared radiation, which is not visible to the naked eye, converting it into images. This technology offers an effective way to determine the surface body temperature. However, depending on the environmental conditions, absolute measurements can be challenging [3].

These cameras convert infrared radiation into electrical signals that are processed into thermograms, which include temperature values and thermal representation. This technique has been used in various fields, including environmental, industrial, and medical studies, especially in thermoregulation, breast cancer detection, neonatal monitoring, urology, and vascular diseases [13].

Infrared thermography is unique due to its non-invasive and contactless nature, being used in medicine and scientific research [11], [19]. It is worth noting that, in thermography, several influences need to be considered, such as physical properties of the examined surface and external environmental factors, as well as external sources of infrared radiation and radiation background [19].

Regarding the measurement of body temperature, thermal imaging offers a way to reduce risks and discomforts associated with skin sensor, allowing the identification of the region that best represents the patient's body temperature [21]. Infrared thermography has proven to be a promising technique in medicine, especially in the monitoring of new-borns and patients in critical conditions. However, it is important to consider its limitations and influences that can affect the accuracy of the measurement to ensure the appropriate interpretation of the data [3], [19], [21].

2.4. Bayesian Networks

Bayesian Networks are a type of probabilistic graphical model that uses concepts from probability theory and graph theory to model uncertainties in complex systems [22]. One of the many applications of Bayesian networks is in regression analysis, where the goal is to predict the response variable based on one or more predictor variables.

In this context, Bayesian networks, with their graphical and probabilistic formalism, prove to be an effective tool for modelling and representing complex relationships, being able to capture linear and non-linear relationships, as well as interactions between predictor variables [23]. This is particularly useful in scenarios where the relationships between variables are complex and perhaps not easily captured by traditional regression techniques.

Bayesian regression incorporates uncertainty both in the regression parameters and in the model structure. This is achieved using prior distributions for the regression parameters and a learning procedure that updates these priors based on the observed data [24]. This results in a posterior distribution for the parameters that captures the remaining uncertainty after the observation of the data. Furthermore, Bayesian networks also allow the incorporation of expert knowledge into the modelling process, which can improve the interpretability of the models and provide better predictions [25]. These features make Bayesian networks an attractive option for regression analysis in many applications.

III. Material and Methods

3.1. Image Database

To capture the images, a thermal camera of model MTV-2010 from Minipa[1] manufacturer was used. This camera generates a visible (RGB) and thermal image side by side, as shown in Figure 2. Another important feature to highlight from the camera is the operating range for temperature measurement, being -10°C to +350°C with an accuracy: ±2°C and resolution of 0.1°C. The emissivity has a selection option between 0.10 and 1.00 with compensation for ambient temperature reflection.

In the composition of the image database, the temperature was also recorded using a contact thermometer, popularly known as a forehead thermometer. This served as a reference device for collecting the temperature and comparing it with the measurement made through the thermal image. This thermometer has an operating temperature range between 34°C and 42.2°C, with resolution: 0.1°C and accuracy: +0.2°C.

To conduct the experiments, 460 thermal images were acquired, with two images being captured for each acquisition. For each volunteer, an image capture was performed with the recording of the reference temperature (with the forehead thermometer) before capture. Then, the person cleans their facial cheeks with a paper towel, and a new capture is made, also with the reference temperature recorded before capture. Figure 2 shows an example of what this image looks like.

[1] https://www.minipa.com.br/images/Manual/MTV-120%20-1102M-BR.pdf

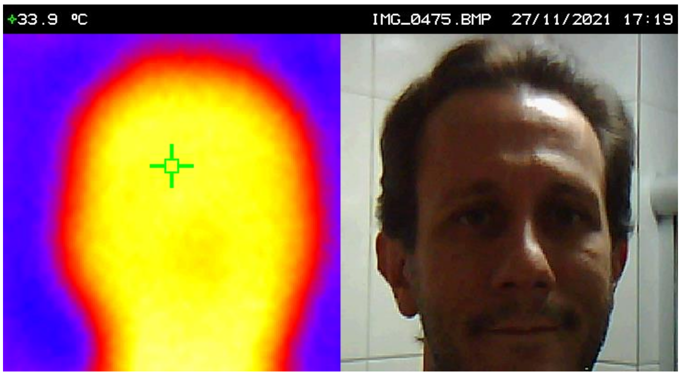

Figure 2. Example of the captured .BMP image

This procedure of cleaning the facial cheeks with a paper towel was to eliminate possible traces of oiliness, this task proved necessary since the capture before and after cleaning can generate variations of up to 0.3ºC, being a deficiency of the infrared image capture system. Table 1 presents an example of the data generated by these captures.

Table 1. Sampling of data obtained from collected images.

File	Thermometer Temperature	Camera Temperature	Error
img_0001	36.8	31.1	-5.7
img_0002	36.4	31.0	-5.4
img_0004	36.4	29.9	-6.5
img_0005	36.4	30.0	-6.4
img_0007	36.2	29.8	-6.4
img_0008	36.1	30.1	-6.0
img_0010	36.2	29.2	-7.0
img_0011	35.7	29.2	-6.5
img_0013	36.1	30.2	-5.9
img_0014	36.1	30.1	-6.0
img_0015	36.4	29.3	-7.1
img_0016	35.9	29.3	-6.6
img_0017	36.1	29.3	-6.8
img_0018	35.8	29.4	-6.4
img_0020	36.1	29.3	-6.8

As can be observed in Table 1, the errors measured directly by the thermal camera in relation to the contact digital thermometer are quite high, which makes it unfeasible for use as a tool for monitoring tasks that require precision. Figure 3 shows some examples of thermal images that were used in this experiment.

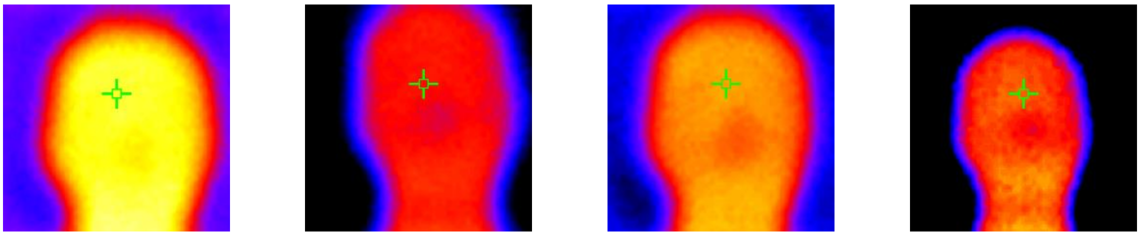

img_0001 img_0002 img_0003 img_0004

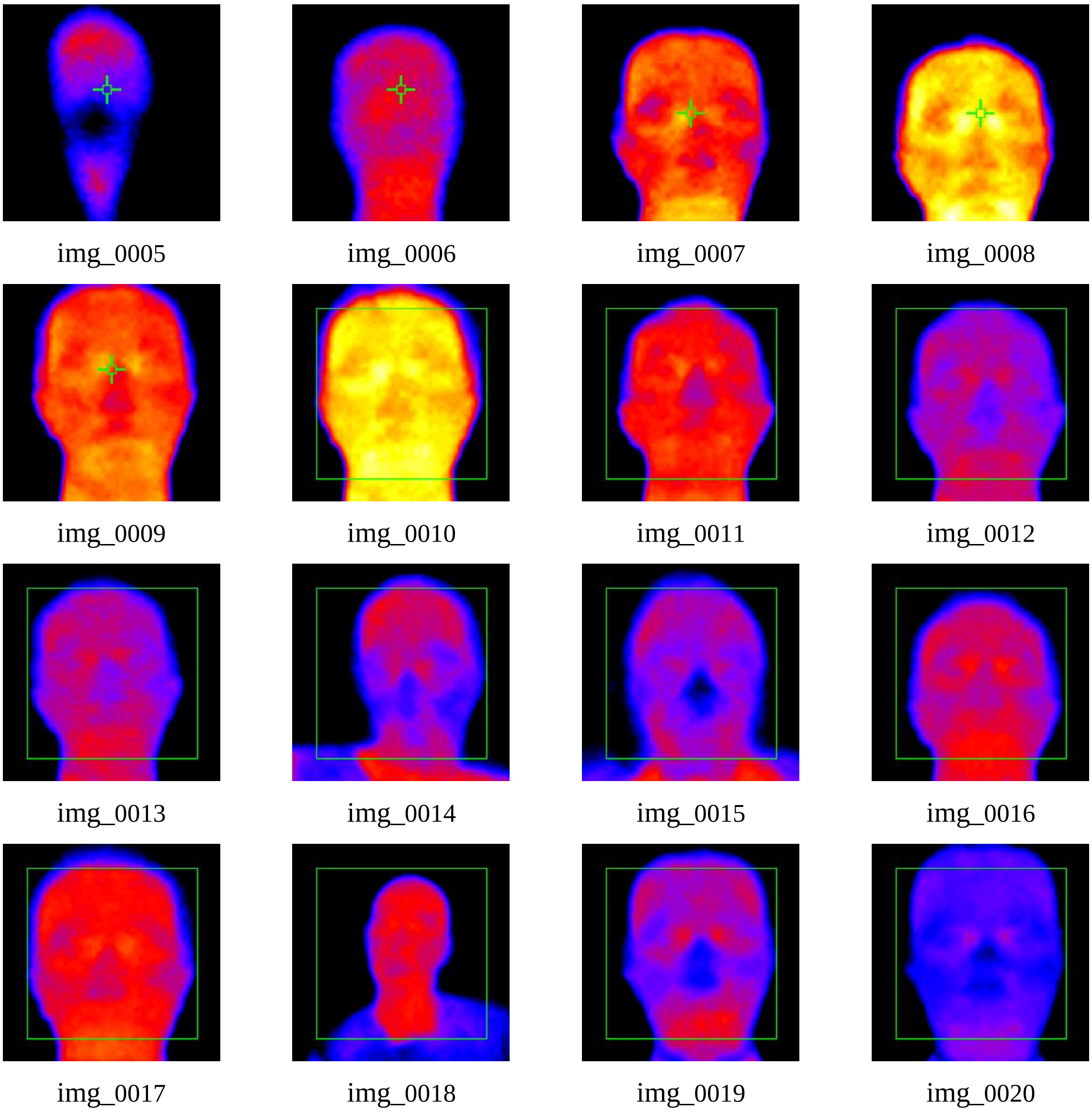

Figure 3. Example of the captured .BMP image

3.2. Proposed Methodology

The proposed methodology for conducting the experiments used the MATLAB® application with the Regression Leaner toolbox, as it is possible to validate the best regression approach for the presented problem. The choice of this language was favoured by the existence of tools for image processing and machine learning already implemented.

The diagram presented in Figure 4 contains the steps of the process from image capture to processing and display of the results. In the diagram, the image acquisition part is the process used to form the image database.

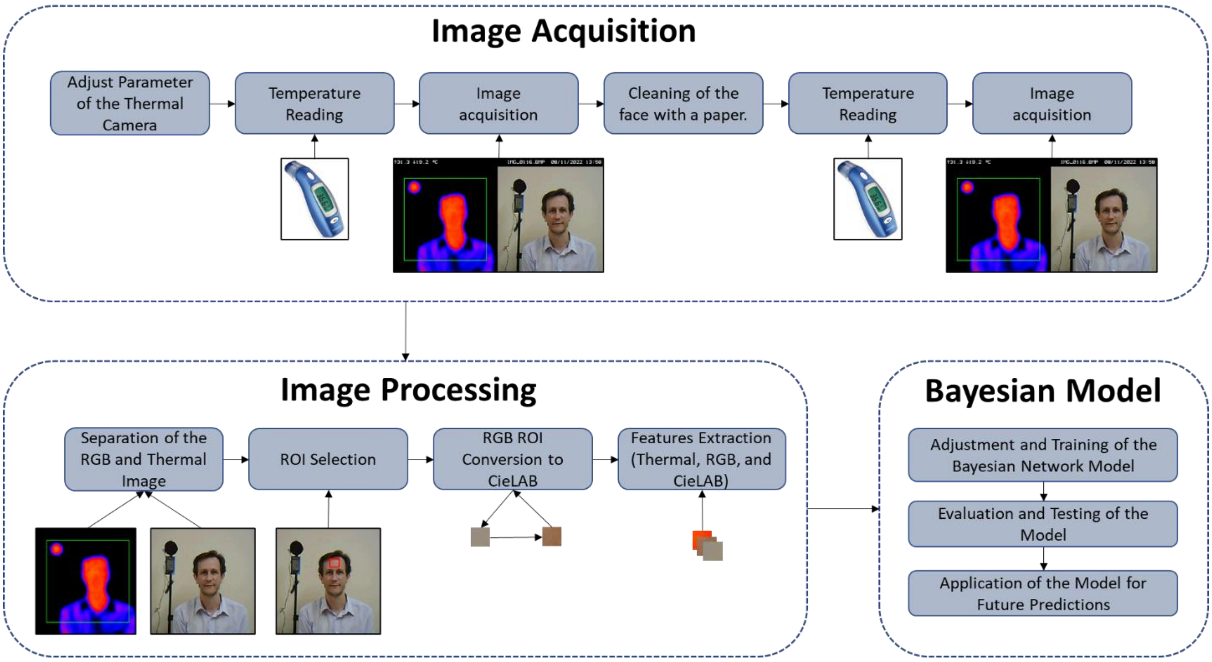

Figure 4. Diagram for the proposed methodology

Next, each block of the diagram presented in Figure 4 will be explained in detail.

1. Image Acquisition: This block contains all the steps of the image acquisition process to create the image database. The same process should be used for new captures and future predictions.
    a. Adjust parameters of Thermal Camera: at this point, all adjustments are made to the thermal camera to meet the needs presented by the problem.
    b. Temperature Reading: At this point, the temperature in the person's forehead region is measured using a contact thermometer.
    c. Image acquisition: at this point, the first image of the person is captured by the camera.
    d. Cleaning of the face with a paper: this step is necessary because skin oiliness surface should cause reading errors. Thus, with two images, the algorithm can learn to compensate for this problem.
    e. Temperature Reading: At this point, the temperature in the person's forehead region is measured again using a contact thermometer.
    f. Image acquisition: In this step the second image of the person is captured by the camera.
2. Image Processing: In image processing, the pre-processing steps and feature extraction are executed.
    a. Separation of the RGB and Thermal Image: This step consists of opening the .BMP file from the camera and dividing it into two new images, the first being the image with the thermal temperature representation and the second the visible RGB image of the person.
    b. ROI Selection: the process of selecting the ROI (Region of Interest) involves cropping a 20x20 pixel window from the forehead region, both from the RGB image and the thermal image, thus generating two new images.
    c. RGB ROI Conversion to CieLAB: To be able to perceive skin oiliness, the RGB ROI was converted to the CIE Lab color space, as such color space is composed of brightness information, which is very useful in this analysis.

   d. Extraction of Features from the ROI (Thermal RGB, Visible RGB, and CieLAB): The extraction of ROI features involves extracting the values of the RGB bands from the thermal and visible ROIs and the Lab bands from the CIE Lab ROI. In addition to band values, the temperature of the thermal ROI is also calculated based on the color distribution and camera specifications, thus performing a direct conversion, the same way as performed by the software provided by Minipa.

3. Bayesian Network

   a. Adjustment and Training of the Bayesian Network Model: the first step to be performed was the adjustment of the hyperparameters of the Bayesian network through the Gaussian regression process (GRP) available in MATLAB. This process was the most satisfactory for the available training data. The Grid Search method was also used but did not obtain parameters as good as the ones presented. It is worth mentioning that of the total of 460 images available in the image database, 15% of these images were separated for validation in the training process and another 15% were used for the tests, leaving 70% or 322 images for training.

   b. Evaluation and Testing of the Model: once the Bayesian network was trained, the test data from the 69 samples reserved for this purpose was presented, each one containing 10 attributes, RGB bands of the thermal and visible ROIs, Lab bands of the CIE Lab ROI, and temperature extracted from the thermal image. At this moment, all evaluation metrics presented in the discussion of results were calculated.

   c. Application of the Model for Future Predictions: At this stage, it is possible to capture a new image going through all previous steps until obtaining the temperature prediction, as well as presenting previously obtained data for its prediction.

The collection of thermal images was carried out in adult individuals for the development of the temperature extraction method. Thermal images of black bodies (temperature reference equipment) for camera stability verification were also acquired, thus serving to validate the use of the thermal camera used in this research.

Before capturing images and collecting data, it is essential to ensure the correct configuration of the camera, including parameters such as alignment between the thermal and visible image, emissivity adjustment, focus, distance, and others. The process of image capture and data collection involves two main stages:

- Collect pre-capture data: includes recording parameters such as identification, temperatures measured with the reference thermometer, and the camera's thermal scale.
- Capture thermal and visible images: involves recording both images in the camera's memory, which is set to store the thermal image and visible image in a single .bmp file.

The collected data are recorded on a spreadsheet, which also identifies the respective images. Once the data and images are stored and correctly identified, they can be processed using the developed computational approach.

It's worth mentioning that for the captures, the focus configuration was set at a distance of 1m, as far as several tests this distance demonstrated to be more adequate. The emissivity must be set at 0.98 (this emissivity is associated with the emissivity of human skin). The camera cursor was set to the window mode and the range was manually adjusted between 24,2°C and 35,5°C. This lower range was adjusted because, as demonstrated on table 1, the camera presented a significant offset error, where a reasonable normal body temperature value, around 36°C, corresponds to approximately 30°C indicated by the camera. The range adjustment optimizes the use of the thermal range to extract RGB values from the thermal image. The camera used in the study stores the data from the thermal image and visible image in two file formats:

- .BMP extension - File with the captured infrared (IR) and visible image and arranged side-by-side with image details at the top;
- .IR2 extension - Specific file of the camera software that allows access to captured infrared data. It was not possible to access this data. For this reason, a specific code to process the BMP file and capturing RGB values in the thermal image was developed.

IV. Results and Discussion

The results obtained from the application of the proposed methodology revealed several and significant observations. A total of 460 thermal images were analysed, and the implementation of the algorithm in MATLAB enabled efficient extraction of relevant data.

The errors measured directly from the thermal camera compared to the digital contact thermometer showed an average of 4.6°C with a standard deviation of 0.95°C. This significant difference highlights the need for calibration and adjustment for the use of the camera in applications that require precision.

The proposed methodology applied a Bayesian network with hyperparameters adjusted through the Gaussian regression process. During the training of the algorithm, a determination coefficient (R-squared) of 0.23164°C was observed, indicating that approximately 23.16% of the temperature variation on the predicted values by the model. In the test data, the determination coefficient was slightly lower, recording 0.20578°C.

After the implementation of the Bayesian network algorithm, a significant reduction in the average error was observed. With an average of 0.16°C and a mean squared error deviation of 0.042°C, the result indicates that the proposed methodology was able to considerably improve the precision of the thermal camera's measurements.

Furthermore, the results indicated that cleaning the skin before image capture can influence temperature measurements, leading to variations of up to 0.3°C on the thermal image. This aspect highlights the importance to consider the cleaning situation of the skin surface in future studies and in the practical application of infrared thermography.

Another important information is the distribution and maximum deviations (prediction errors) observed after the training process. These deviations range was between -0.73°C and +0.51°C in the test set. This variation is represented in Figure 5 with the distribution of predictions by temperature.

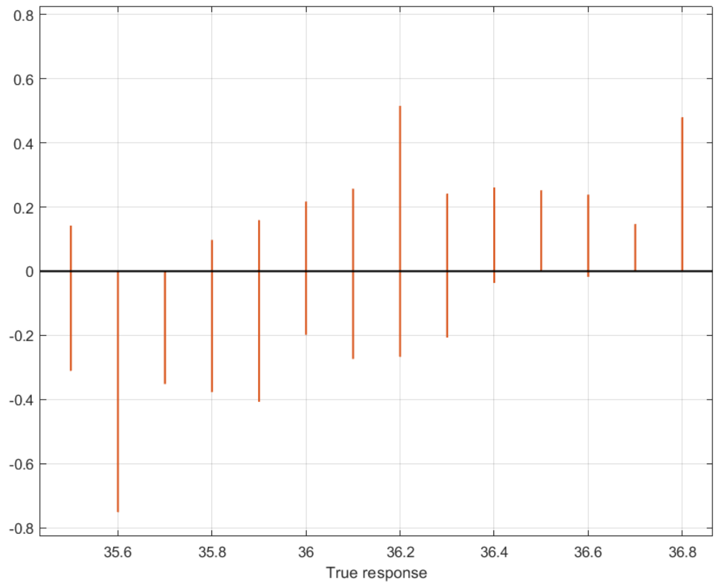

Figure 5. Diagram for the proposed methodology

Figure 6 presents the evolution of the Bayesian network training process, illustrating the evolution of the Minimum Mean Squared Error (MSE) as the training progressed. The results show a stabilization of the training, and the point is presented where the configuration hyperparameters were obtained, also representing the lowest MSE. It is worth to mention that the hyperparameters obtained at this point are stored for future predictions.

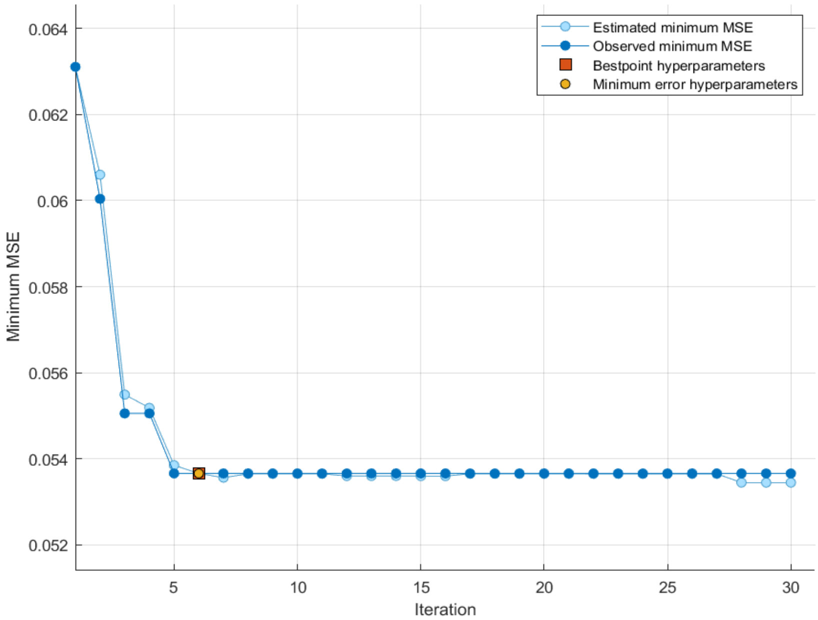

Figure 6. Evolution of the Bayesian network training process (GRP)

In summary, the results obtained demonstrate significant progress towards improving the precision of temperature measurements made by the thermal camera and the feasibility of the proposed methodology for measuring body temperature. However, the results still need to be improved for applications that require more precise measurements for body temperature, such as in the case of monitoring in the healthcare area.

V. Conclusions

This study provided an in-depth look at the application of Bayesian networks in the analysis of thermal images for accurate body temperature measurement. The results obtained offer a significant advancement over traditional temperature measurement methods, mainly due to the minimization of the error observed in the thermal camera's measurements.

The use of a carefully designed methodology, which involved camera calibration, temperature verification with a contact thermometer, image capture and processing, as well as the application and training of a Bayesian network model, allowed for more accurate and reliable results.

While the results still need to be improved for applications requiring more accurate measurements, such as health area monitoring, the proposed methodology has proven to be a promising solution for body temperature measurement. It stands out for its ability to compensate for reading errors caused by skin oiliness, as well as enabling the efficient use of infrared thermography for image acquisition.

Future work can focus on improving the accuracy of the Bayesian network model and experimenting with different parameters for better optimization. Furthermore, the incorporation of more data into the image database can enhance the model's ability to make accurate predictions.

In conclusion, this study offers an important step towards improving the accuracy of temperature measurements of thermal cameras available on the market. The proposed methodology provides a viable solution for accurately measuring body temperature and serves as a basis for future research in this domain.

Acknowledgements

The authors would like to thank Nove de Julho University by financial support and the scholarship provided to Edward Netzer.

REFERENCES

[1] R. A. Joseph, S. Derstine, M. Killian, and S. Gephart, "Ideal site for skin temperature probe placement on infants in the NICU," *Advances in Neonatal Care*, vol. 17, no. 2, pp. 114–122, 2017.

[2] S. Sollai *et al.*, "Performance of a non-contact infrared thermometer in healthy newborns," *BMJ Open*, vol. 6, no. 3, p. e008695, 2016.

[3] A. K. Abbas, K. Heimann, K. Jergus, T. Orlikowsky, and S. Leonhardt, "Neonatal non-contact respiratory monitoring based on real-time infrared thermography," *Biomed Eng Online*, vol. 10, no. 1, pp. 1–17, 2011.

[4] K. Ammer and F. Ring, *The thermal human body: a practical guide to thermal imaging*. CRC Press, 2019.

[5] R. P. Clark and J. K. Stothers, "Neonatal skin temperature distribution using infra-red colour thermography.," *J Physiol*, vol. 302, no. 1, pp. 323–333, May 1980, doi: 10.1113/JPHYSIOL.1980.SP013245.

[6] L. Hanssler and H. Breukmann, "Hauttemperaturmessungen bei Frühgeborenen," *Klin Padiatr*, vol. 204, no. 05, pp. 355–358, Sep. 1992, doi: 10.1055/s-2007-1025371.

[7] A. K. Abbas and S. Leonhardt, "Intelligent neonatal monitoring based on a virtual thermal sensor," *BMC Med Imaging*, vol. 14, no. 1, p. 9, Dec. 2014, doi: 10.1186/1471-2342-14-9.

[8] F. J. Rodriguez-Lozano, F. León-Garc\'\ia, M. de Adana, J. M. Palomares, and J. Olivares, "Non-invasive forehead segmentation in thermographic imaging," *Sensors*, vol. 19, no. 19, p. 4096, 2019.

[9] T. Negishi *et al.*, "Contactless vital signs measurement system using RGB-thermal image sensors and its clinical screening test on patients with seasonal influenza," *Sensors*, vol. 20, no. 8, p. 2171, 2020.

[10] F. Yang, S. He, S. Sadanand, A. Yusuf, and M. Bolic, "Contactless measurement of vital signs using thermal and RGB cameras: A study of COVID 19-related health monitoring," *Sensors*, vol. 22, no. 2, p. 627, 2022.

[11] R. B. Knobel-Dail, D. Holditch-Davis, R. Sloane, B. D. Guenther, and L. M. Katz, "Body temperature in premature infants during the first week of life: Exploration using infrared thermal imaging," *J Therm Biol*, vol. 69, pp. 118–123, 2017.

[12] E. A. Berksoy, Ö. Bağ, S. Yazici, and T. Çelik, "Use of noncontact infrared thermography to measure temperature in children in a triage room," *Medicine*, vol. 97, no. 5, 2018.

[13] A. H. Ornek, M. Ceylan, and S. Ervural, "Health status detection of neonates using infrared thermography and deep convolutional neural networks," *Infrared Phys Technol*, vol. 103, p. 103044, 2019.

[14] K. Rassels and P. French, "Accurate Body Temperature Measurement of a Neonate Uusing Thermography Technology," in *2021 Smart Systems Integration (SSI)*, 2021, pp. 1–5.

[15] M. A. Jaddoa, L. Gonzalez, H. Cuthbertson, and A. Al-Jumaily, "Multiview eye localisation to measure cattle body temperature based on automated thermal image processing and computer vision," *Infrared Phys Technol*, vol. 119, p. 103932, 2021.

[16] F.-K. Wang, J.-Y. Shih, P.-H. Juan, Y.-C. Su, and Y.-C. Wang, "Non-invasive cattle body temperature measurement using infrared thermography and auxiliary sensors," *Sensors*, vol. 21, no. 7, p. 2425, 2021.

[17] Thomas Jung *et al.*, "Light Sensitivity," Sep. 2008. Accessed: Jun. 04, 2023. [Online]. Available: http://ec.europa.eu/health/ph_risk/risk_en.htm

[18] M. A. Akhloufi and A. Bendada, "Fusion of active and passive infrared images for face recognition," in *Thermosense: Thermal Infrared Applications XXXV*, SPIE, May 2013, p. 87050B. doi: 10.1117/12.2017942.

[19] V. Bernard, E. Staffa, V. Mornstein, and A. Bourek, "Infrared camera assessment of skin surface temperature–effect of emissivity," *Physica Medica*, vol. 29, no. 6, pp. 583–591, 2013.

[20] M. Charlton *et al.*, "The effect of constitutive pigmentation on the measured emissivity of human skin," *PLoS One*, vol. 15, no. 11, p. e0241843, 2020.

[21] C. H. Antink *et al.*, "Fast body part segmentation and tracking of neonatal video data using deep learning," *Med Biol Eng Comput*, vol. 58, pp. 3049–3061, 2020.

[22] J. Pearl, *Probabilistic reasoning in intelligent systems: networks of plausible inference*. Morgan kaufmann, 1988.

[23] D. Koller and N. Friedman, *Probabilistic graphical models: principles and techniques*. MIT press, 2009.

[24] C. M. Bishop and N. M. Nasrabadi, *Pattern recognition and machine learning*, vol. 4, no. 4. Springer, 2006.

[25] D. Heckerman, D. Geiger, and D. M. Chickering, "Learning Bayesian networks: The combination of knowledge and statistical data," *Mach Learn*, vol. 20, pp. 197–243, 1995.

Authors

Edward Netzer, PMP certified Project Manager, Higher Education Professor and Electronic Engineer. Master's student in Knowledge Management and Artificial Intelligence, Specialist in Project Management from FGV (Fundação Getulio Vargas), former member of PMI (Project Management Institute) with PMP certification (Project Management Professional) and Electronic Engineer graduated from Escola de Engenharia Mauá. Expertise in project management for the development of electronic products with experience in medical electrical equipment (neonatology, anesthesia, ventilation and monitoring), automotive electronics (window lifters and alarms) and power electronics (UPS and AVR). Acting as a Professor in human subjects aimed at the executive career and in exact subjects aimed at the technical career in the area of Electronics. He currently works with Project Management and development of electromedical equipment at FANEM. Has experience in the areas of Project Management, Process Management, Research and Development, Electronic Engineering and Product Development

Peterson Belan, PhD in Informatics, Master in Production Engineering and Bachelor in Computer Science from Nove de Julho University. Professor of the Graduate Program in Informatics and Knowledge Management and collaborating professor of the Bachelor's Degree in Electrical Engineering at UNINOVE. He has worked on the following research topics: Image Processing and Computer Vision, Computational Intelligence, IoT-Internet of Things, Smart Cities, Metaheuristic Algorithms, Machine Learning, System and Process Optimization. Experience in Computer Science, with emphasis on programming and image processing, automation of metrological processes and device development.